CBPF-NF-062/01

Influence of low-lying discrete nuclear states on isotopic abundances in presupernova cores

A. Dimarco, C. Barbero
Centro Brasileiro de Pesquisas Físicas
Rua Dr. Xavier Sigaud 150, 22290-180 Rio de Janeiro-RJ, Brazil

H. Dias
Instituto de Física, Universidade de São Paulo
C.P. 66318, 05315-970 São Paulo-SP, Brazil

F. García
Departamento de Ciências Exatas e Tecnológicas,
Universidade Estadual de Santa Cruz,
Km 16, Rodovia Ilhéus-Itabuna,
45650-000 Ilhéus-Ba, Brazil

J. Horvath
Instituto Astronômico e Geofísico
Universidade de São Paulo
C.P. 3386 01060-970, 01060-970 São Paulo-SP, Brazil

L. Losano
Departamento de Física, Universidade Federal de Paraíba,
C.P. 5008, 58059-110 João Pessoa-PB, Brasil

The influence of low-lying discrete nuclear states on isotopic abundances in presupernova core is discussed. Assuming the hypothesis of nuclear statistical equlibrium (NSE) the Saha equation has been solved for a set of 65 nuclear species (including free protons and neutrons). Experimental data have been used in the calculation of the first terms of the nuclear partition function. The obtained abundances are compared with those evaluated using an energy level density in the computation of the nuclear partition function. We conclude that in future calculations involving isotopic abundances in presupernova core, the low-lying nuclear states need to be treated as discrete ones, when experimental data are available.

PACS number(s): 26.45, 95.30.C, 97.10.C, 97.60

I. INTRODUCTION

Except for few light elements, originating from the Big Bang, all heavier elements are made in stellar evolution and stellar explosions [1]. Massive stars [2–5] that grow "iron" cores live $\tau \sim 7 \times 10^6 (M/10M_\odot)^{-3} yr$ burning hydrogen. The next nuclear reactions are successively the fusion of He, C, Ne, O and Si. Burning continues up to ^{56}Fe, which is the nucleus with the highest binding energy per nucleon [6]. The progress in understanding the synthesis of iron-group nuclei has been in a broadening of the picture of possible statistical equilibria and how nature realizes these equilibria. The idea of statistical equilibrium [7–10] has played a special role in the history of stellar nucleosynthesis theory. Hoyle [11] recognized that the dramatic peak in the abundances of the iron-group nuclei called for synthesis under conditions of temperature and density such that statistical equilibrium was attained between nuclei and free neutrons and protons, and he showed that evolved stars reached appropriate thermal conditions. We have assumed in this work that after silicon burning [12] is completed, the strong and electromagnetic reactions are in equilibrium in the "iron" core [13]. It is important to clarify that it is not completly true because there may not be time for beta decays to establish NSE before collpase intervenes. Nuclear weak processes (e.g., beta decays and electron capture) are not in equilibrium because the inverse reaction to beta decay requires the absorption of neutrinos, and these escape freely from the star during presupernova evolution . At this point, the NSE is characterized by only three variables: density (ρ), temperature (T) and electron fraction (Y_e) [14]. The nuclear Saha equation gives the abundance of the each nuclear specie as a function of these three variables plus the binding energy and partition function of each nucleus [7,13]. In this way, accurate values of the nuclear partition function are an important ingredient in the determination of the isotopic abundances in the presupernova environment. Nuclear partition function plays an important role in other astrophysical scenarios. It also appears in the abundances isotopics calculations in silicon burning [12], in the determination of equation of state during gravitational collapse [15,16], etc.

Epstein and Arnett [8] have used the ground state ($G = 2J_0 + 1$, with J_0 being the ground state spin), but as the temperature increases the nuclear partition function becomes quite different from $(2J_0 + 1)$. In Ref. [13] all the excited states were taken into account through a level density integral. The nuclear partition function for a nucleus of mass A is conventionally obtained by considering the Boltzman population of a Fermi gas-nuclear state density [17,18]. The rapid growth of this density with excitation energy U ($\sim U^{-5/4} \exp(\sqrt{2aU})$, where $a \approx A/8$ MeV^{-1}) results in an extremely large partition

function at temperatures of only a few MeV. On the other hand, some works [19,20] point out that the statistical treatment usually does not give an adequate description of the level density at low energies.

As pointed out in a recent work [21], the low-lying discrete nuclear states should be treated using the available experimental data. The authors concludes that the difference between the experimental low-lying levels distribution and the calculated level density can lead to an important distortion of the nuclear partition function. Some works in the literature remark the importance of low-lying discrete nuclear states in other astrophysical environment. Among these we mention the Ref. [22], about the calculation of reaction rates ($< \sigma v >$) in the r-process, and the Ref. [12] about the physic of quasi-equlibrium in the silicon burning phase.

The aim of this work is to study the influence of the low-lying discrete nuclear states on the isotopic abundances in a presupernova environment, under the assumption of NSE. Particular attention is devoted to analyze the deviation obtained when a level density is used in the description of those states.

This paper is organized as follows. In Sec. II we summarize the equation needed to obtain the isotopic abundances. Numerical results are presented and discussed in Sec. III. We close with some conclusions in Sec. IV.

II. CALCULATIONS

After silicon burning is completed in the "iron" core, the Saha equation gives the isotopic abundance of each nuclear specie. If $\mathcal{N}$ nuclides (including protons and neutrons) are considered, there will be $\mathcal{N}-2$ equations [7],

$$\frac{n_{\mathsf{A,Z}}}{G_{\mathsf{A,Z}}(T)}\left(\frac{2\pi\hbar^2}{A m_{\mathsf{H}} k_{\mathsf{B}} T}\right)^{\frac{3}{2}} = \frac{n_{\mathsf{p}}^{\mathsf{Z}} n_{\mathsf{n}}^{(\mathsf{A}-\mathsf{Z})}}{2^{\mathsf{A}}}\left(\frac{2\pi\hbar^2}{m_{\mathsf{H}} k_{\mathsf{B}} T}\right)^{\frac{3\mathsf{A}}{2}} \exp\frac{B_{\mathsf{A,Z}}}{k_{\mathsf{B}} T}, \tag{1}$$

where n_{p} and n_{n} are the density of free protons and neutrons, $n_{\mathsf{A,Z}}$ is the density* of the nuclear specie ${}^{\mathsf{Z}}\mathrm{A}$, $G_{\mathsf{A,Z}}(T)$ is the nuclear partition function, $B_{\mathsf{A,Z}}$ is the binding energy, m_{H} is the hydrogen atom mass, and the all other constants have the usual meaning. Assuming that nuclear reactions occur so rapidly that no weak processes are able to occur, then only two further equations are required. They specify the density,

*The densities n_{p}, n_{n} and $n_{\mathsf{A,Z}}$ are expressed in units of number of particles per unit of volume.

$$\rho = \sum_{\mathsf{A,Z}} A n_{\mathsf{A,Z}} m_{\mathsf{H}} + (n_{\mathsf{p}} + n_{\mathsf{n}})\, m_{\mathsf{H}}, \tag{2}$$

and the ratio of total number of protons to neutrons,

$$R = \frac{\sum_{\mathsf{A,Z}} Z n_{\mathsf{A,Z}} + n_{\mathsf{p}}}{\sum_{\mathsf{A,Z}} (A - Z) n_{\mathsf{A,Z}} + n_{\mathsf{n}}}. \tag{3}$$

The electron fraction and R are related by

$$R = \frac{Y_{\mathsf{e}}}{1 - Y_{\mathsf{e}}}, \tag{4}$$

because of the electric charge conservation.

For each value of Y_{e}, we have calculated numerically the abundances of the nuclei in statistical equilibrium by solving the the equations (1), (2) and (3) by the standard methods [7]. The respective value of ρ and T has been obtained following the stellar trajectory fitted by Aufderheide et al [13] given by:

$$\log_{10} \rho\,(Y_{\mathsf{e}}) = 603 - 3642 Y_{\mathsf{e}} + 7439 Y_{\mathsf{e}}^2 - 5075 Y_{\mathsf{e}}^3 \tag{5}$$

and

$$T_9(Y_{\mathsf{e}}) = 1212 - 7571 Y_{\mathsf{e}} + 15831 Y_{\mathsf{e}}^2 - 11047 Y_{\mathsf{e}}^3, \tag{6}$$

where T_9 is the stellar temperature in units of $10^9\ K$. These equations are valid for stars with mass between 15 and 25 $M_\odot$.

In ours calculations we have used two different approximations for the nuclear partition function [21]. In the first one the low-lying states are treated as discrete:

$$G^{(\mathsf{D+C})}_{\mathsf{A,Z}}(T) = G^{(\mathsf{D})}_{\mathsf{A,Z}}(T) + \int_{\mathsf{E_D}}^{\infty} dE \int_0^{\infty} dJ (2J+1) \Phi(E,J) \exp\left(-\frac{E}{k_{\mathsf{B}} T}\right), \tag{7}$$

where

$$G^{(\mathsf{D})}_{\mathsf{A,Z}}(T) = \sum_{\mathsf{m=0}}^{\mathsf{E_D}} (2J_{\mathsf{m}} + 1) \exp\left(-\frac{E_{\mathsf{m}}}{k_{\mathsf{B}} T}\right), \tag{8}$$

with $\Phi(E,J)$ being the nuclear level density and E_{D} is the cut off energy. Here we have used the level density introduced by Gilbert and Cameron [24]. The sum in equation (8) goes up to $E_{\mathsf{D}} \simeq 3$ MeV. We have chosen this value taking into account the strong attenuation of the exponential factor for energies > 3 MeV, at temperatures of interest [21]. When the experimental available information is up to energies < 3 MeV, the E_{D} value

is the bigger available experimental svalue[†]. Similar expressions for the nuclear partition function can be found in [15,16], but in theses works the discrete sum is truncated in the first term as in Ref. [8].

In the second approximation the low-lying nuclear states contribution is included by means of the same level density:

$$G^{(\mathsf{C})}_{\mathsf{A},\mathsf{Z}}(T) = 2J_0 + 1 + \int_0^\infty dE \int_0^\infty dJ(2J+1)\Phi(E,J)\exp\left(-\frac{E}{k_{\mathsf{B}}T}\right). \tag{9}$$

Binding energies, $B_{\mathsf{A},\mathsf{Z}}$, of all nuclear have been taken from Ref [23].

III. RESULTS AND DISCUSSIONS

We have calculated the densities n_{n} and n_{p} of free protons and neutrons, and the density $n_{\mathsf{A},\mathsf{Z}}$ for the set of 63 nuclear species which we show in Fig. 1. We have included in our calculation the most relevant isotopes present in presupernova core environment [13]. The isotopic abundances, defined as $x_{\mathsf{A},\mathsf{Z}} = Am_{\mathsf{H}}n_{\mathsf{A},\mathsf{Z}}\rho^{-1}$, are plotted in Figs 2-7 for the Ca, Sc, Ti, V, Cr, Mn, Fe, Co, Ni, Cu and Zn nuclei, as a function of the electron fraction. Similarly, the free proton and neutron abundances $x_{\mathsf{s}} = m_{\mathsf{H}}n_{\mathsf{s}}\rho^{-1}$ $(s = n, p)$ are shown in Fig. 8. In all these figures we present the results for both aproximations of the nuclear partition function: $G^{(\mathsf{D}+\mathsf{C})}_{\mathsf{A},\mathsf{Z}}(T)$ (solid line) and $G^{(\mathsf{C})}_{\mathsf{A},\mathsf{Z}}(T)$ (dashed line). We can see that, at presupernova conditions, the isotopic abundances are very sensitive to the approximation used for the nuclear partition function, which shows clearly the importance of the low-lying discrete states. In Table I we show the direct impact of the low-lying discrete nuclear states on the abundances calculation for a few cases. The ^{57}Fe abundance increases in a factor ~ 4 for $Y_{\mathsf{e}} = 0.457$, $\rho = 7.19 \times 10^7$ and $T_9 = 3.97$. In the case of ^{64}Ni, the abundance is reduced in a factor ~ 2 for $Y_{\mathsf{e}} = 0.434$, $\rho = 3.90 \times 10^8$ and $T_9 = 4.86$.

In order to analize these differences more quantitatively, we define the parameters $\varepsilon_{\mathsf{A},\mathsf{Z}}$ and ε_{s} $(s = n, p)$:

$$\varepsilon_{\mathsf{A},\mathsf{Z}} \equiv 100 \times \frac{\log_{10} x^{(\mathsf{C})}_{\mathsf{A},\mathsf{Z}} - \log_{10} x^{(\mathsf{D}+\mathsf{C})}_{\mathsf{A},\mathsf{Z}}}{\log_{10} x^{(\mathsf{D}+\mathsf{C})}_{\mathsf{A},\mathsf{Z}}} \tag{10}$$

and

[†]Excitation energies, E_{m}, can be found in http://www.nndc.bnl.gov/nndc/nudat

$$\varepsilon_{\mathsf{s}} \equiv 100 \times \frac{\log_{10} x_{\mathsf{s}}^{(\mathsf{C})} - \log_{10} x_{\mathsf{s}}^{(\mathsf{D+C})}}{\log_{10} x_{\mathsf{s}}^{(\mathsf{D+C})}}, \tag{11}$$

where the superscripts $(D+C)$ and (C) denote that the isotopic abundances were calculated using the partition functions $G_{\mathsf{A,Z}}^{(\mathsf{D+C})}$ and $G_{\mathsf{A,Z}}^{(\mathsf{C})}$, respectively. This parameter mesures the error introduced in the isotopic abundance order of magnitude when we use the level density $\Phi(E,J)$ to describe the low-lying discrete nuclear states. In Figs. 9-14 we show $\varepsilon_{\mathsf{A,Z}}$ as a function of the electron fraction, for Ca, Sc, Ti, V, Cr, Mn, Fe, Co, Ni, Cu and Zn. In Fig. 15 we plot ε_{p} and ε_{n}. Figs. 9-11 show errors of 20 % for ^{50}Ca, ^{51}Sc, ^{52}V and ^{56,57}Mn isotopes at presupernova conditions. Some isotopes of iron, cobalt and nickel (e.g. ^{59,61}Fe, ^{58}Co and ^{63,64}Ni) also present errors around of 20 %, as we can see in Figs. 12 and 13. A singular case is ^{57}Fe (see top graphic of Fig. 12) which have an error of 50 %. With the goal of understand these results we compute the theoretical accumulated number of levels N(E) given by:

$$N(E) = 2J_0 + 1 + \int_0^{\mathsf{E}} dE' \int_0^{\infty} dJ(2J+1)\,\Phi(E',J). \tag{12}$$

In Fig. 16 we compare the theoretical and experimental accumulated number of levels $N(E)$ for ^{57}Fe. The big difference between $x_{57,26}^{(\mathsf{C})}$ and $x_{57,26}^{(\mathsf{D+C})}$ originates in the very low energy-value (14.4 keV) of the first excited state of ^{57}Fe. The contribution of this state to the first term of $G_{57,26}^{(\mathsf{D+C})}(T)$, (see equations (7) and (8)) is very important at temperatures of presupernova environment. We have a similar situation for ^{58}Co in Fig. 17. In the ^{64}Ni case the theoretical accumulated number of levels is greater than the experimental one, as can be seen in Fig. 18, and $x_{64,28}^{(\mathsf{C})} > x_{64,28}^{(\mathsf{D+C})}$, which means that $\varepsilon_{64,28} < 0$. In most of the cases in which the theoretical accumulated number of levels is larger (smaller) than the experimental one, we get $x_{\mathsf{A,Z}}^{(\mathsf{C})} > x_{\mathsf{A,Z}}^{(\mathsf{D+C})}$ $\left(x_{\mathsf{A,Z}}^{(\mathsf{C})} < x_{\mathsf{A,Z}}^{(\mathsf{D+C})}\right)$.This last statment is not always true. To give a deeper understanding, suposse that the theoretical accumulated number of levels is greater than the experimental one for all the isotopes. Then the relation $x_{\mathsf{A,Z}}^{(\mathsf{C})} > x_{\mathsf{A,Z}}^{(\mathsf{D+C})}$ can not fullfiled for all nuclei because of mass and charge conservation.

Finally, it is important to realize that in the early stages of precollapse (Y_{e} nearly less than 0.5 and T_9 nearly great than 4) both approximations leads to the same results ($\varepsilon_{\mathsf{A,Z}} \simeq 0$). We can understand this fact if we note that, in this regime of temperature, the contribution of the Boltzman factor to the partition function is very small.

The variation in the abundance of any isotope changes all the others abundances, because they are tied by the mass and charge conservation (see equations (2) and (3)). In order to analize the effect of the discrete low-lying levels of the ^{57}Fe, which is the isotope with the lower first excited state, we define the parameter $\delta_{\mathsf{A,Z}}$ as:

$$\delta_{\mathsf{A,Z}} \equiv 100 \times \frac{\log_{10} x^{(\mathsf{C})}_{\mathsf{A,Z}} - \log_{10} x^{*}_{\mathsf{A,Z}}}{\log_{10} x^{(\mathsf{C})}_{\mathsf{A,Z}}}, \tag{13}$$

where $x^{*}_{\mathsf{A,Z}}$ denotes that the equations (1), (2) and (3) have been solved using $G^{(\mathsf{C})}_{\mathsf{A,Z}}(T)$ for all isotopes except for ^{57}Fe, in which case we have used $G^{(\mathsf{D+C})}_{\mathsf{A,Z}}(T)$. This parameter measures the influence of the first excited state of ^{57}Fe on the isotopic abundance of all the other nuclear species. In Figs. 19 and 20 we plot $\delta_{\mathsf{A,Z}}$ vs. Y_{e} for the Fe-Co, and Ni-Cu isotopes, respectively. The ^{57}Fe presents the larger $\delta_{\mathsf{A,Z}}$ - value, around 32 % ($x^{(\mathsf{C})}_{57,26}$ =1.96 $\times$ 10^{-2} and $x^{*}_{57,26} = 7.04 \times 10^{-2}$) for $Y_{\mathsf{e}} = 0.456$, $\rho = 7.5 \times 10^{7}$ and $T_{9} = 4.00$. This result was to be expected if we recall that the ^{57}Fe partition function has been radically changed by the inclusion of the low-lying discrete states. The abundances of the other isotopes are also affected by the inclusion of the term $G^{(\mathsf{D})}_{\mathsf{A,Z}}(T)$ in the nuclear partition function of ^{57}Fe, but by a smaller fraction ($\leq$ 4 %).

IV. CONCLUSIONS

We have discussed the influence of low-lying discrete nuclear states on isotopic abundances in presupernova environment. The isotopic abundances for a relevant set of 65 nuclear species (including free protons and neutrons) was calculated, by solving the Saha equation for two different approximations for the partition function. In the first one we have treated the low-lying nuclear states as discrete, and in the other one their contribution has been included by means of a level density. The results presented in Figs. 9-15 clearly show the important role played by the low-lying states in the evaluation of the isotopic abundances. The inclusion of $G^{(\mathsf{D})}_{\mathsf{A,Z}}(T)$ in the partition function of the different nuclear species produces a significative modification in the calculated values, which is of the order of $\sim$ 20% for ^{50}Ca, ^{51}Sc, ^{52}V, ^{56,57}Mn and some isotopes of the iron-group, as for example, ^{59,61}Fe, ^{58}Co and ^{63,64}Ni. A singular situation is presented by the ^{57}Fe nuclei, which exhibit a desviation of $\sim$50 %. This arises from the very low energy value of the first excited state (14.4 keV). We conclude that in future calculations involving isotopic abundances at presupernova cores, the low lying nuclear states need to be taken as discrete ones, when experimental information is available. We would like to remark that the abundances obtained in this work differ from those in an actual presupernova core beacuse the assumption of NSE was made. Therefore they can be used as a guides to the sorts of the differences that inclusion of the experimental data on low-lying nuclear levels will make to dynamically calculated abundances.

Isotopic abundances play a very important role in the determination of the temporal variation of the electron fraction [13,25]. Electron capture and beta decay are crucial in later phases of stellar evolution, during the stellar colpase, and in explosive events like Type I and II supernovae, novae, and X-ray burst or processes such r and rp [26–32]. As a massive star approaches to the end point of its evolution, the mass of its collapsing core is largely determined by the efficiency of electron capture and beta decay reactions, that regulate the electron degeneracy pressure which supports the star. By this reason, it is very useful to know the temporal variation of the electron fraction, which can be calculated as $\dot{Y}_{\mathrm{e}} = \Sigma(x_{\mathrm{A,Z}}/A)(\lambda^{\mathrm{bd}}_{\mathrm{A,Z}} - \lambda^{\mathrm{ec}}_{\mathrm{A,Z}})$ where the sum runs over all the relevant nuclear species, $\lambda^{\mathrm{bd}}_{\mathrm{A,Z}}$ ($\lambda^{\mathrm{ec}}_{\mathrm{A,Z}}$) is the beta (electron capture) decay rate of the nucleus ${}^{\mathrm{Z}}\mathrm{A}$ and $x_{\mathrm{A,Z}}$ its isotopic abundance. The modifications that we have obtained in the abundances when the low-lying nuclear states are treated as discrete, could lead to some difference in the variation of the electron fraction. We hope to report on this in a forthcoming publication.

In addition, the electron capture and beta decay rates are very sensitive to the $Q-$value of the reaction. For this reason, it is necessary to have an understanding of the Gamow Teller strength function in both the electron capture and beta decay directions.

Acknowledgments

The authors thank to the Brazilian agencies Centro Latinoamericano de Física (CLAF), Conselho Nacional de Desenvolvimento Científico e Tecnológico (CNPq) and Fundação de Amparo à Pesquisa do Estado de São Paulo (FAPESP) for the partial financial support of this work and to Virginia Trimble for many valuable suggestions.

TABLE I. Isotopic abundances for some nuclear species considered in the calculations.

Nuclear specie	Y_e	$\rho\ (g \times cm^{-3})$	T_9	$x_{A,Z}^{(C)}$	$x_{A,Z}^{(D+C)}$
^{52}V	0.442	2.15×10^{8}	4.53	1.62×10^{-3}	5.06×10^{-3}
^{56}Mn	0.446	1.53×10^{8}	4.34	2.48×10^{-3}	7.69×10^{-3}
^{57}Mn	0.438	2.85×10^{8}	4.68	1.27×10^{-2}	2.92×10^{-2}
^{56}Fe	0.465	5.14×10^{7}	3.83	7.13×10^{-1}	7.46×10^{-1}
^{57}Fe	0.457	7.19×10^{7}	3.97	1.92×10^{-2}	7.23×10^{-2}
^{59}Fe	0.440	2.59×10^{8}	4.63	2.82×10^{-2}	5.50×10^{-2}
^{58}Co	0.467	4.96×10^{7}	3.82	5.62×10^{-4}	2.31×10^{-3}
^{58}Ni	0.483	3.23×10^{7}	3.65	6.98×10^{-1}	6.49×10^{-1}
^{63}Ni	0.446	1.53×10^{8}	4.34	6.13×10^{-3}	1.41×10^{-2}
^{64}Ni	0.434	3.90×10^{8}	4.86	2.04×10^{-1}	1.39×10^{-1}

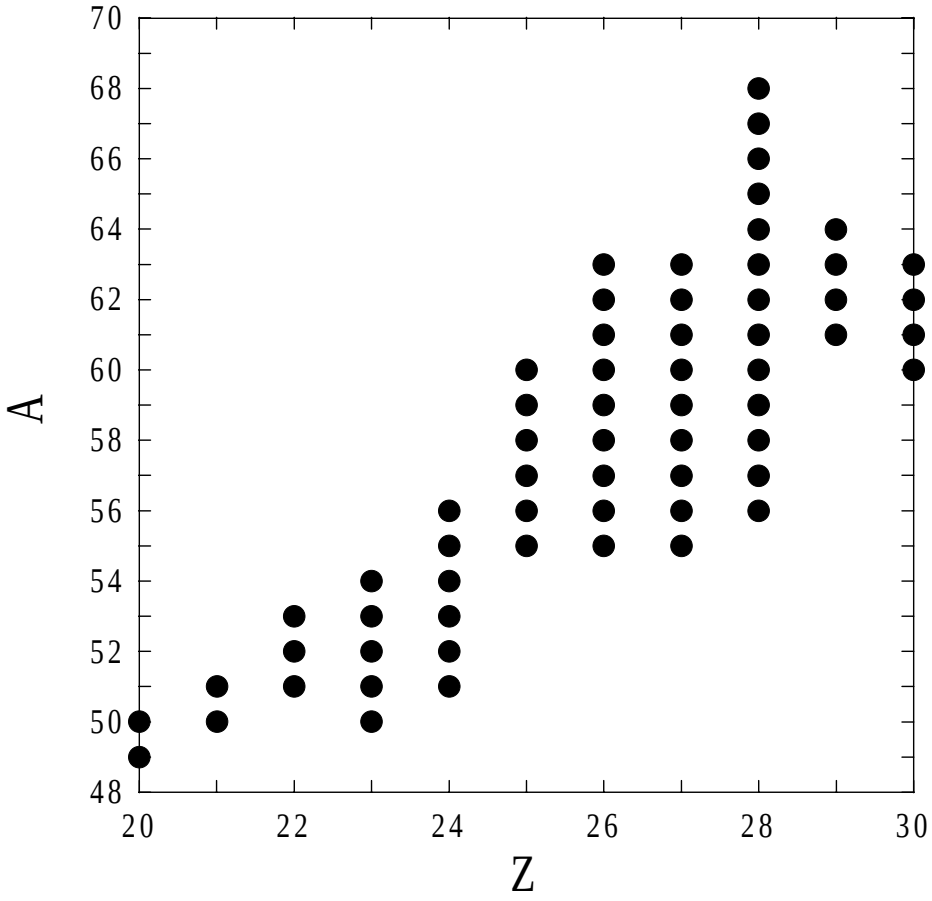

Figure 1
Dimarco et al.

FIG. 1. Nuclei considered in our calculation.

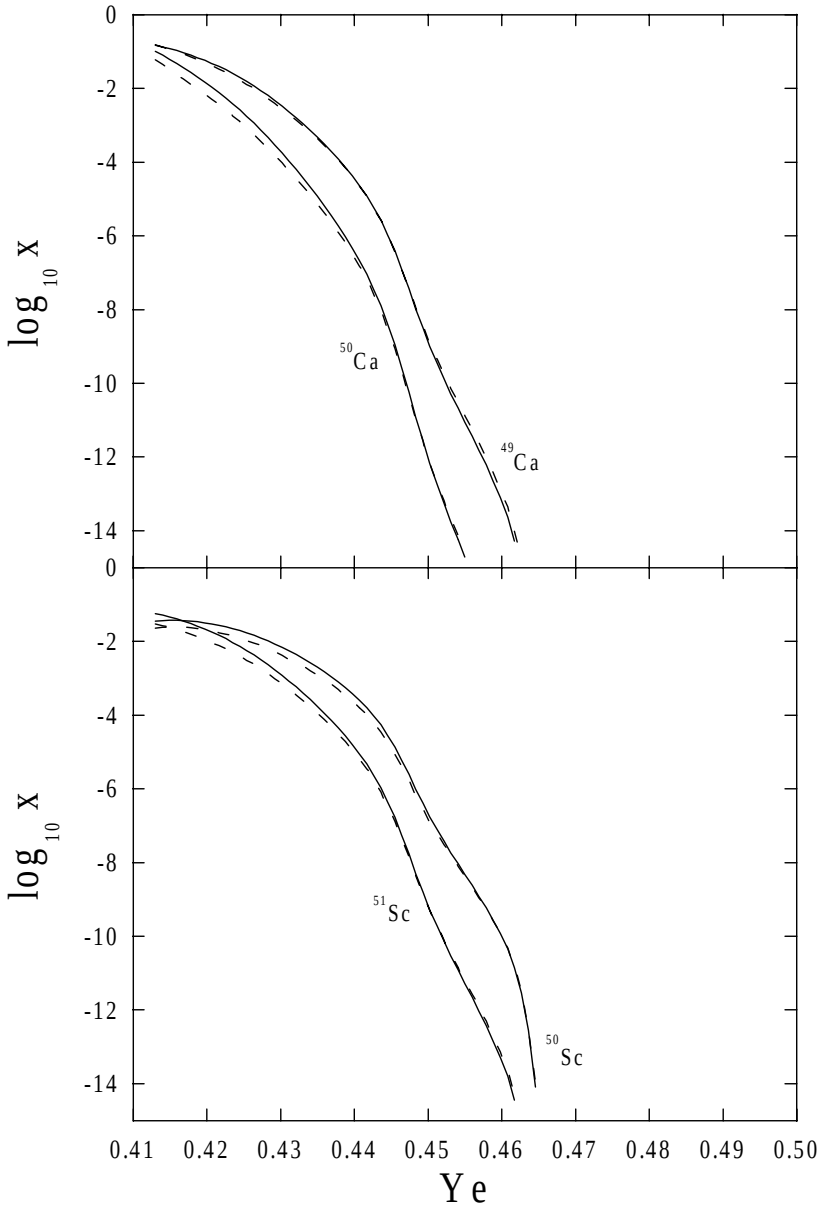

Figure 2
Dimarco et al.

FIG. 2. Isotopic abundances vs. electron fraction for ^{49,50}Ca (top graphic) and $^{50,\,51}$Sc (button graphic). The solid and dashed lines denotes $x_{A,Z}^{(D+C)}$ and $x_{A,Z}^{(C)}$, respectively.

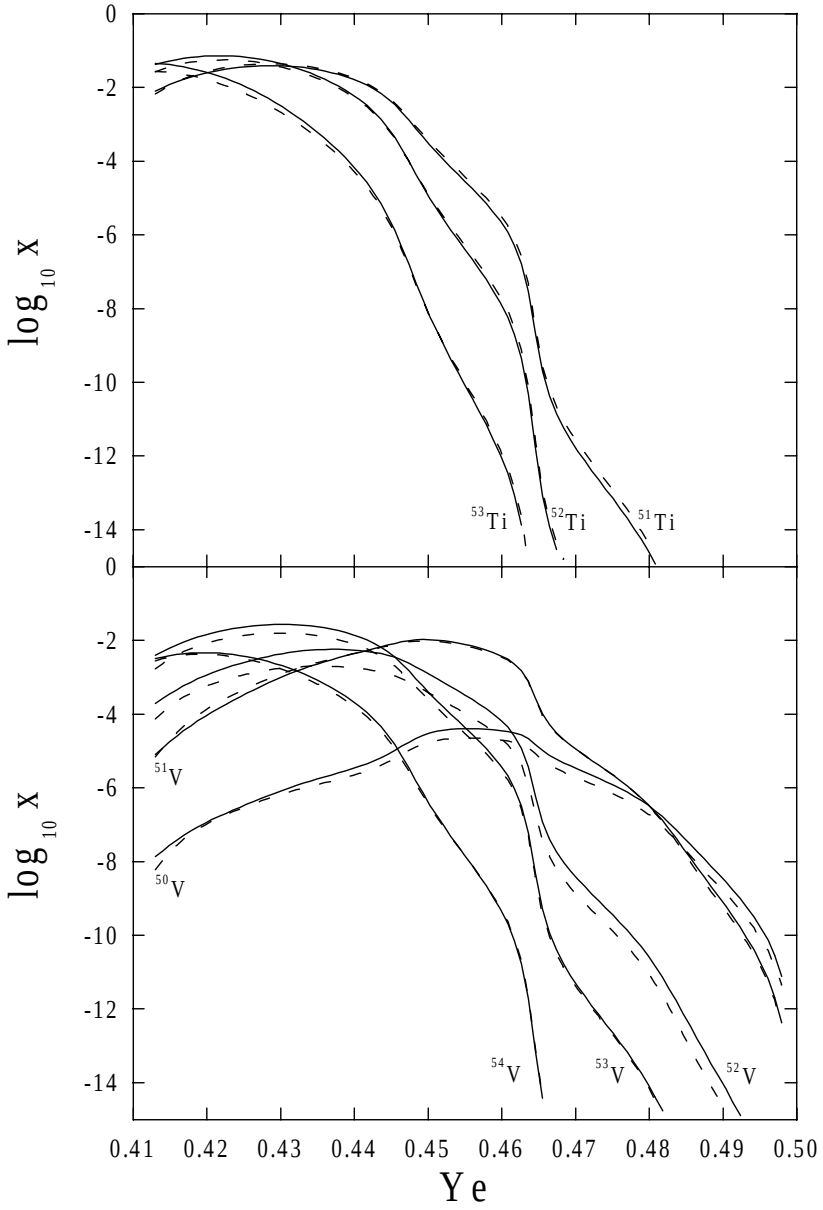

Figure 3
Dimarco et al.

FIG. 3. The same as in Fig. 2 for $^{51,\,52,\,53}$Ti (top graphic) and $^{51,\,52,\,53,\,54}$V (button graphic).

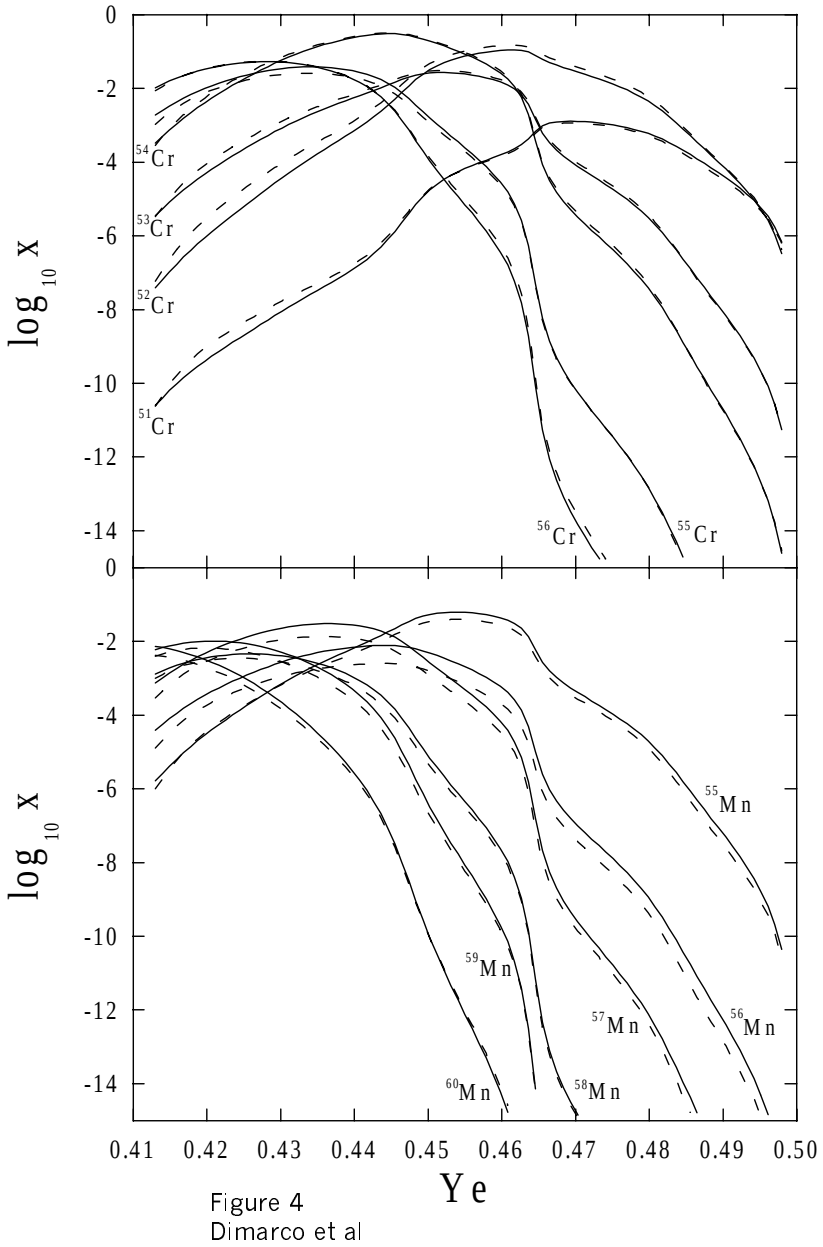

Figure 4
Dimarco et al

FIG. 4. The same as in Fig. 2 for $^{51, 52, 53, 54, 55, 56}$Cr (top graphic) and $^{55, 56, 57, 58, 59, 60}$Mn (button graphic).

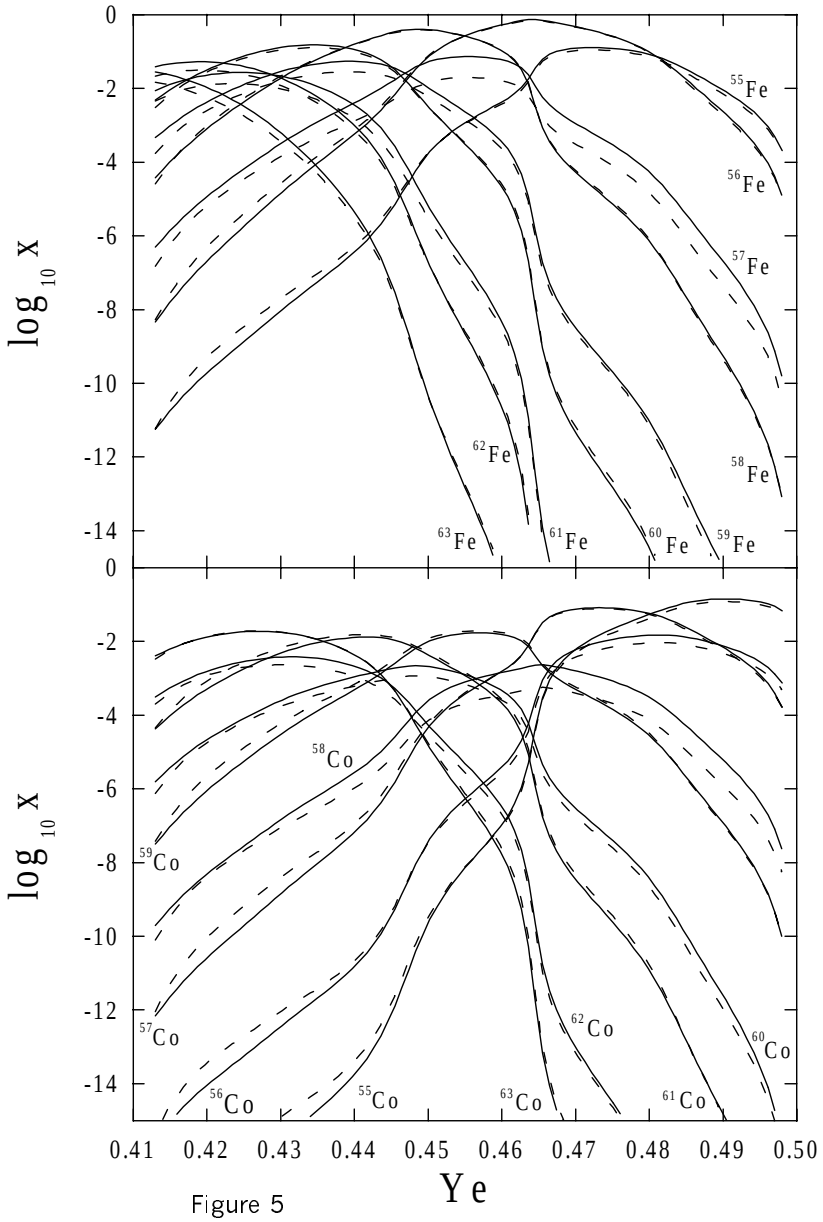

Figure 5
Dimarco et al.

FIG. 5. The same as in Fig. 2 for $^{55, 56, 57, 58, 59, 60, 61, 62, 63}$Fe (top graphic) and $^{55, 56, 57, 58, 59, 61, 61, 62, 63}$Co (button graphic).

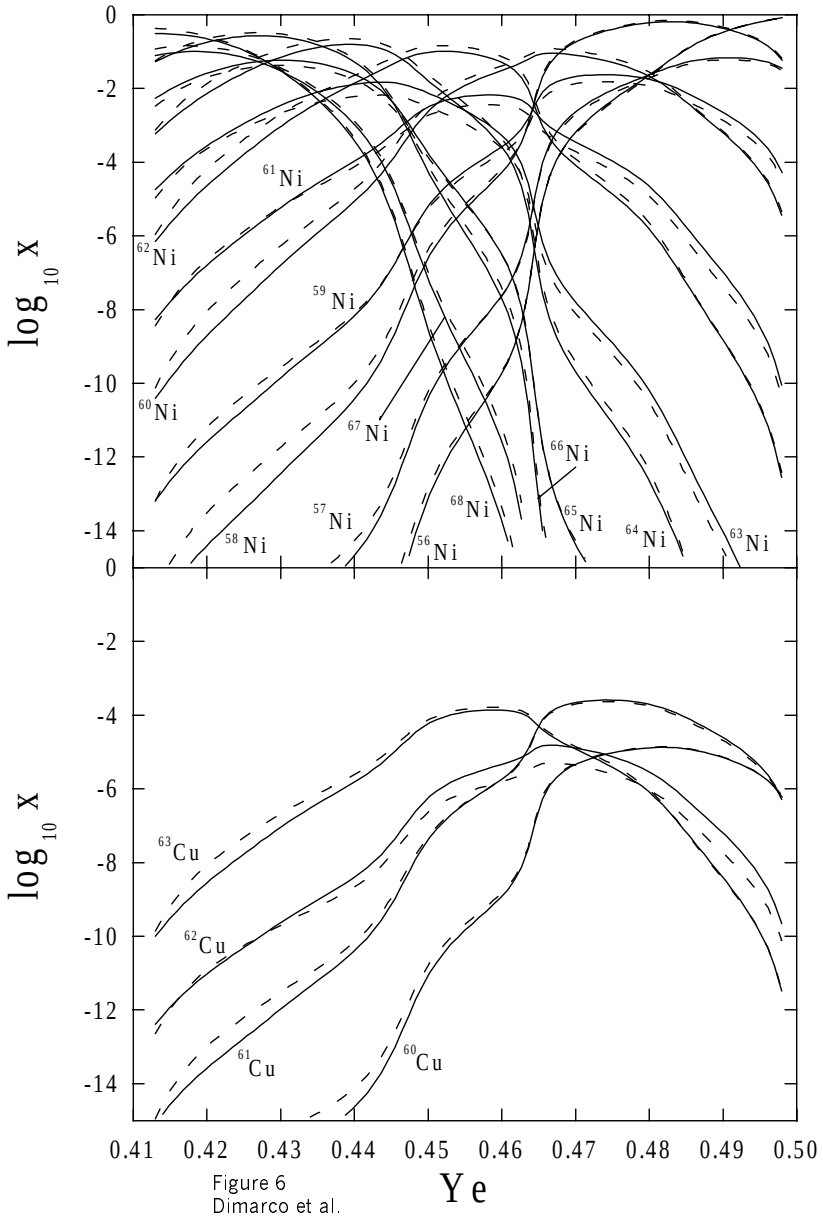

FIG. 6. The same as in Fig. 2 for $^{56,\ 57,\ 58,\ 59,\ 60,\ 61,\ 62,\ 63,\ 64,\ 65,\ 66,\ 67,\ 68}$Ni (top graphic) and $^{60,\ 61,\ 62,\ 63}$Cu (button graphic).

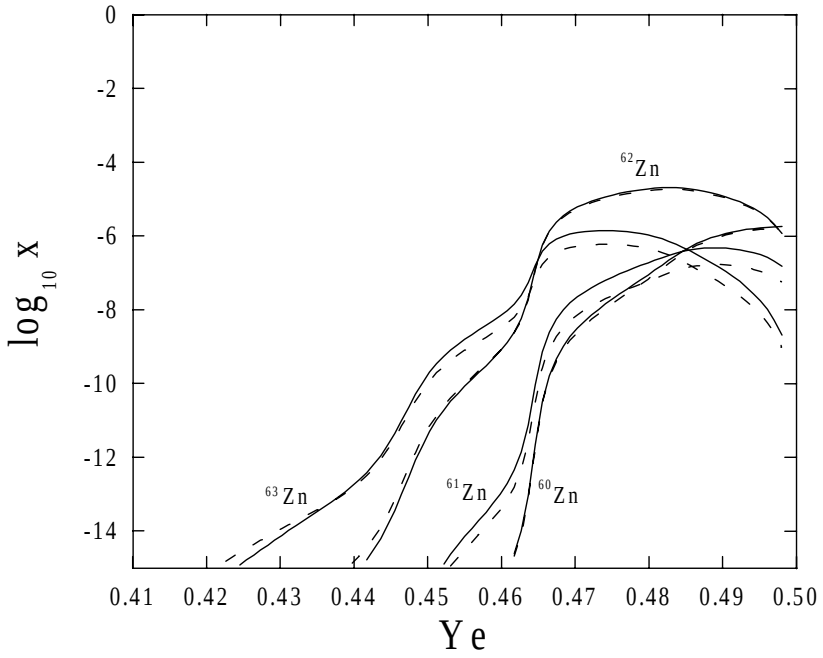

Figure 7
Dimarco et al.

FIG. 7. The same as in Fig. 2 for $^{60,\,61,\,62,\,63}$Zn.

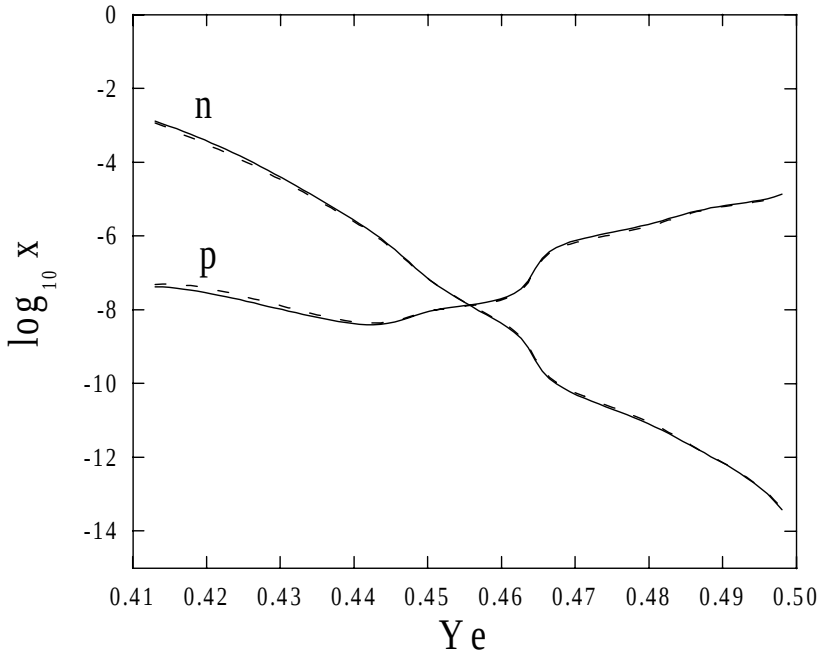

Figure 8
Dimarco et al.

FIG. 8. The same as in Fig. 2 for free protons and neutrons.

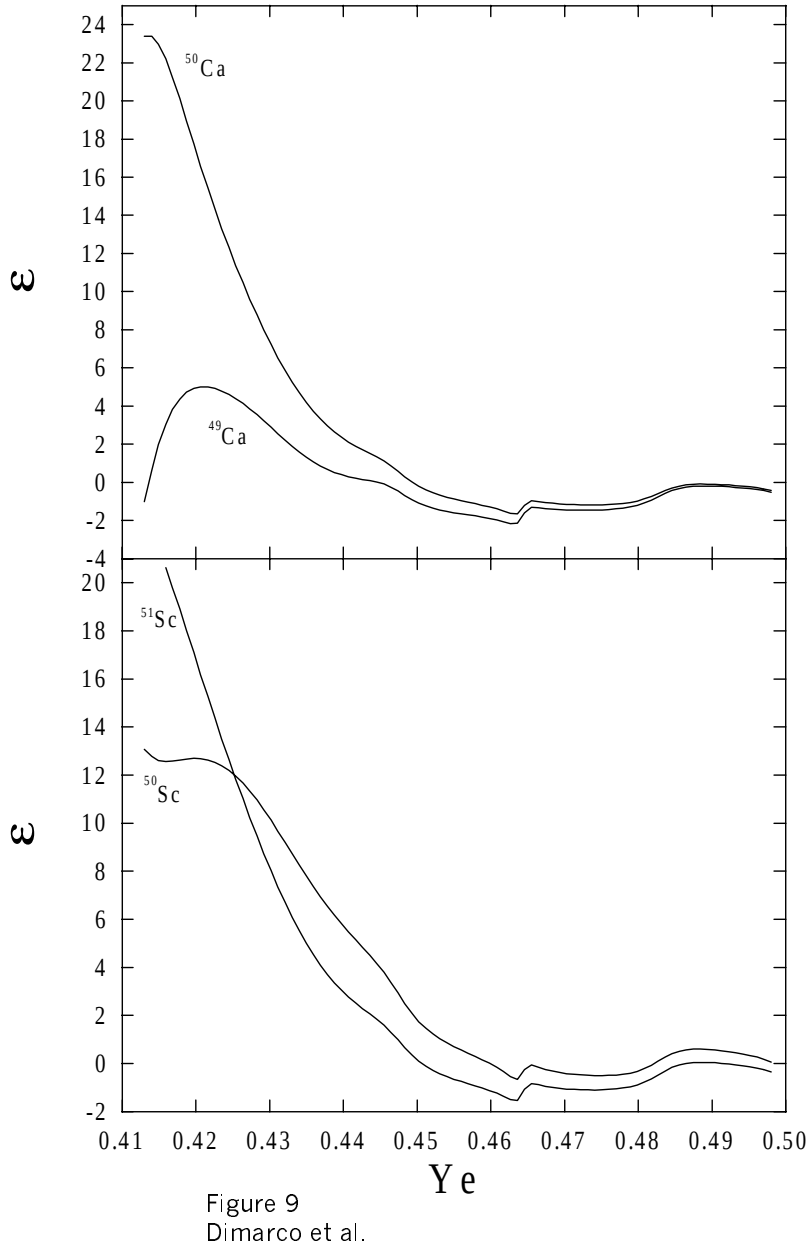

FIG. 9. The parameter $\varepsilon_{A,Z}$ vs. electron fraction for the ^{49,50}Ca (top graphic) and $^{50,\,51}$Sc (button graphic).

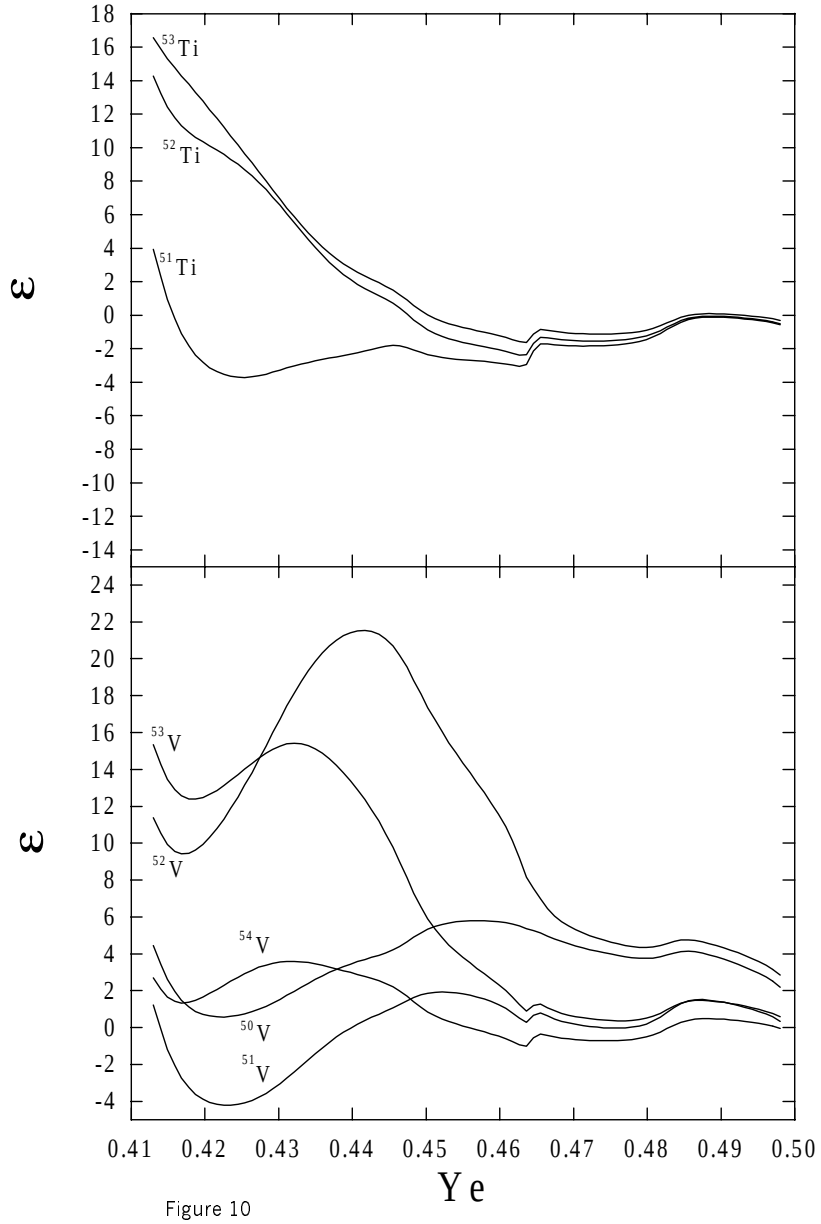

FIG. 10. The same as in Fig. 9 for $^{51,\,52,\,53}$Ti (top graphic) and $^{51,\,52,\,53,\,54}$V (button graphic).

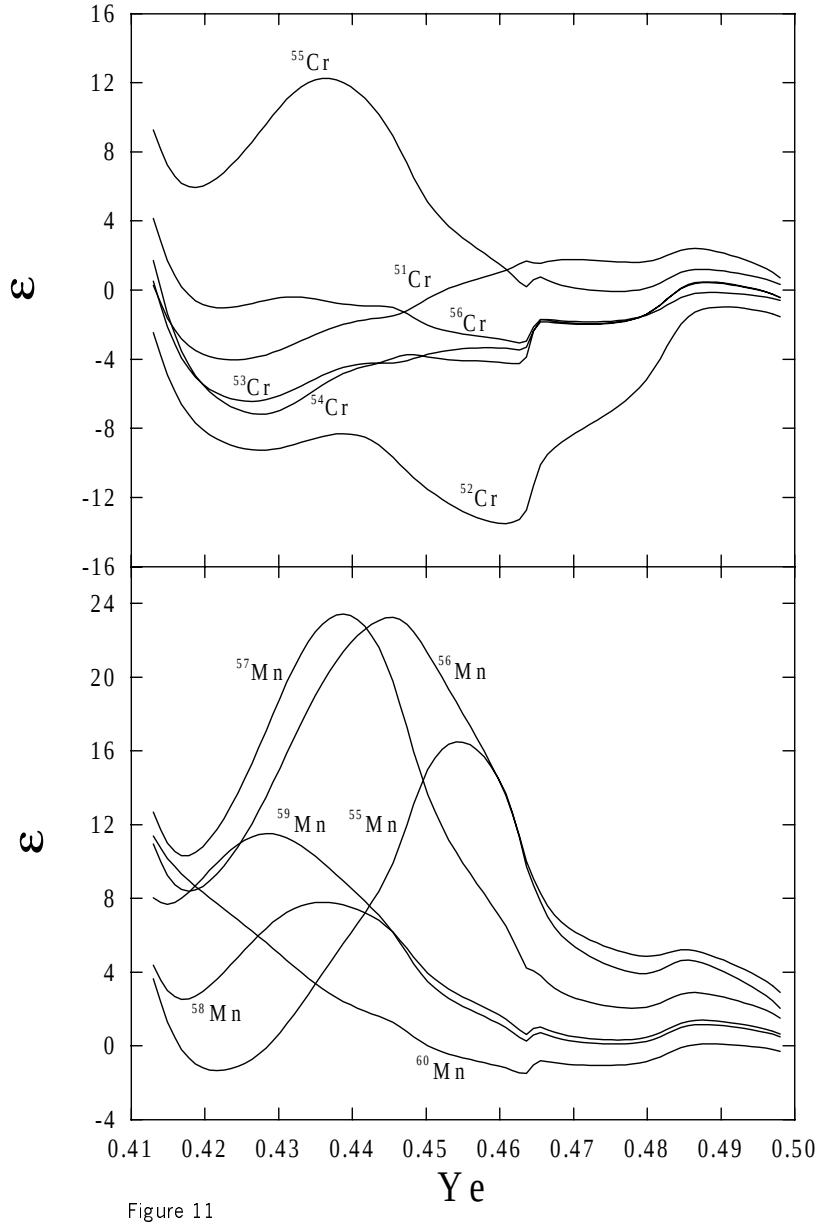

Figure 11
Dimarco et al.

FIG. 11. The same as in Fig. 9 for $^{51, 52, 53, 54, 55, 56}$Cr (top graphic) and $^{55, 56, 57, 58, 59, 60}$Mn (button graphic).

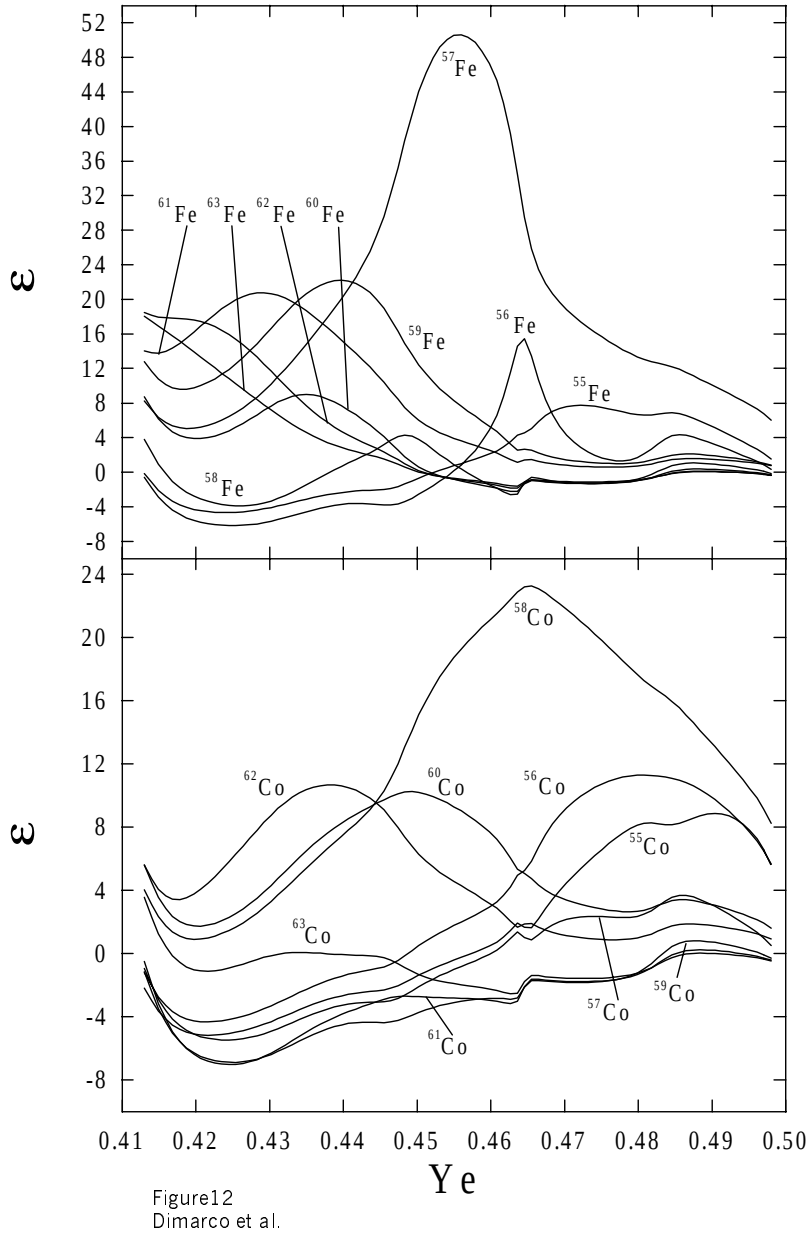

FIG. 12. The same as in Fig. 9 for $^{55, 56, 57, 58, 59, 60, 61, 62, 63}$Fe (top graphic) and $^{55, 56, 57, 58, 59, 60, 61, 62, 63}$Co (button graphic).

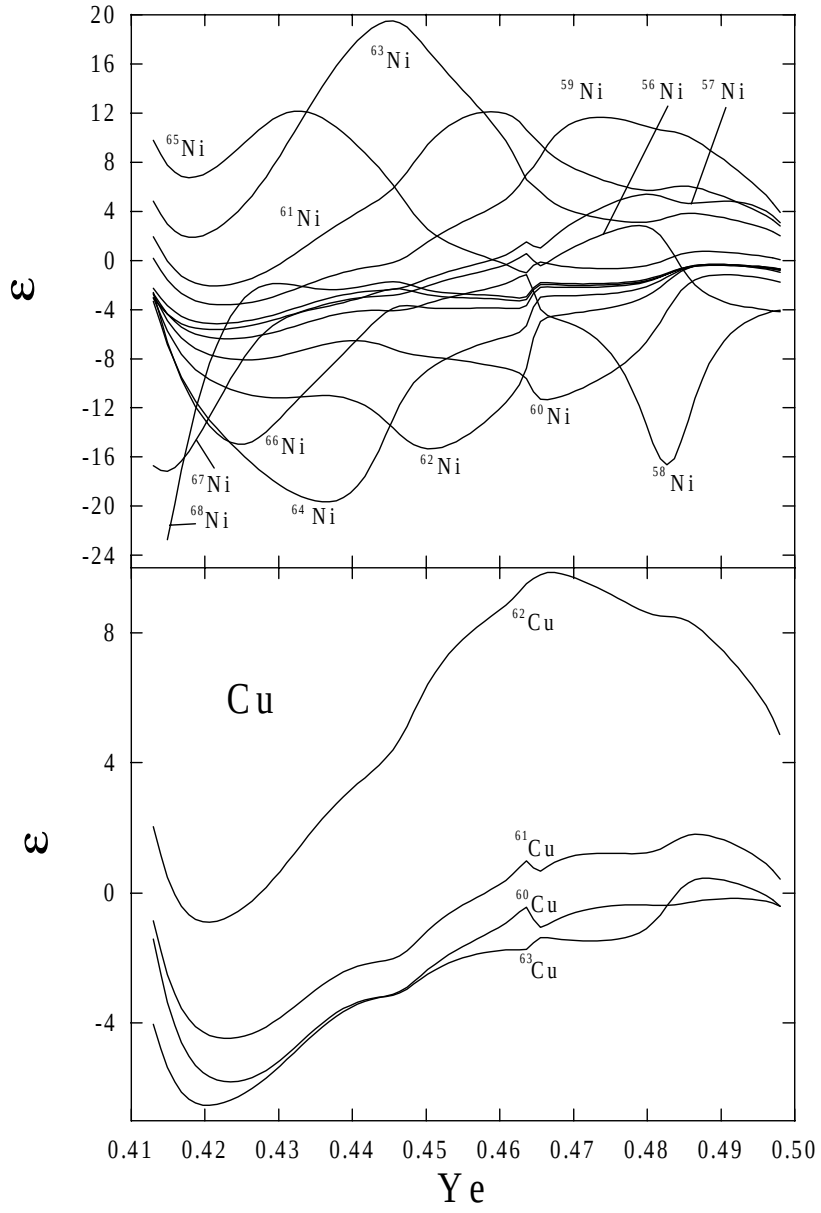

Figure 13
Dimarco et al.

FIG. 13. The same as in Fig. 9 for $^{56, 57, 58, 59, 60, 61, 62, 63, 64, 65, 66, 67, 68}$Ni (top graphic) and $^{60, 61, 62, 63}$Cu (button graphic).

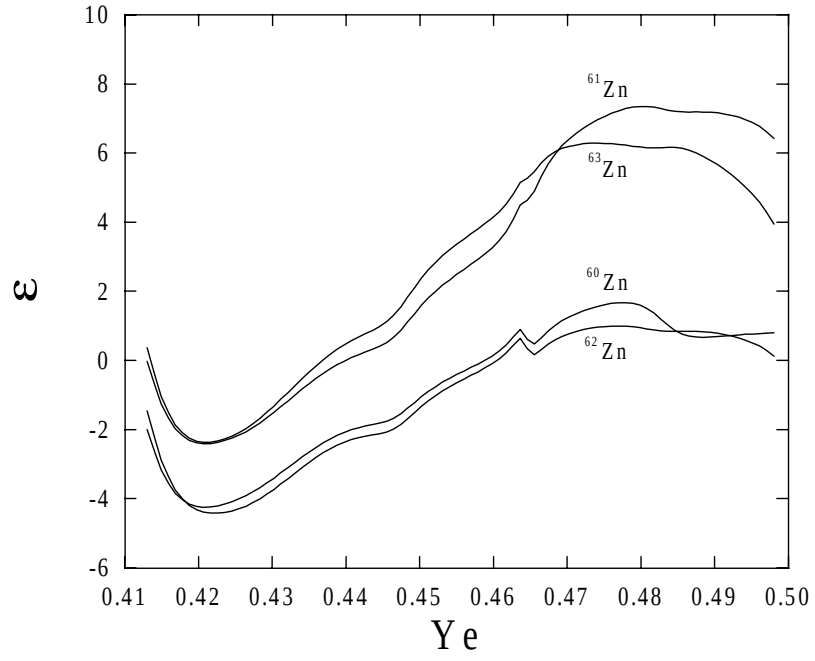

Figure 14
Dimarco et al.

FIG. 14. The same as in Fig. 9 for $^{61,\,62,\,63,\,64}$Zn.

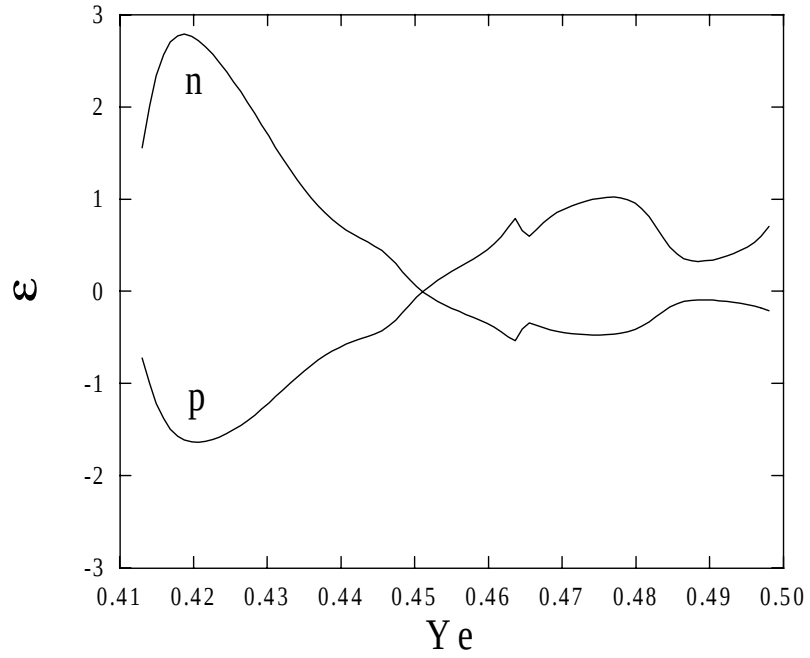

Figure 15
Dimarco et al.

FIG. 15. The same as in Fig. 9 for free proton and neutrons.

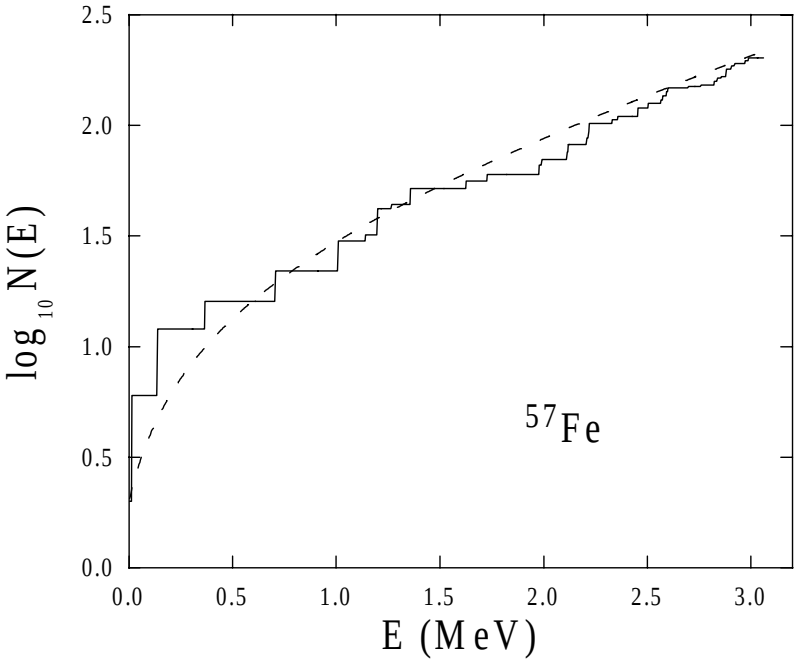

Figure 16
Dimarco et al.

FIG. 16. Accumulated number of levels vs. excitation energy for ^{57} Fe. Solid line denotes experimental data and dashed line denotes theoretical calculations (see equation (12))

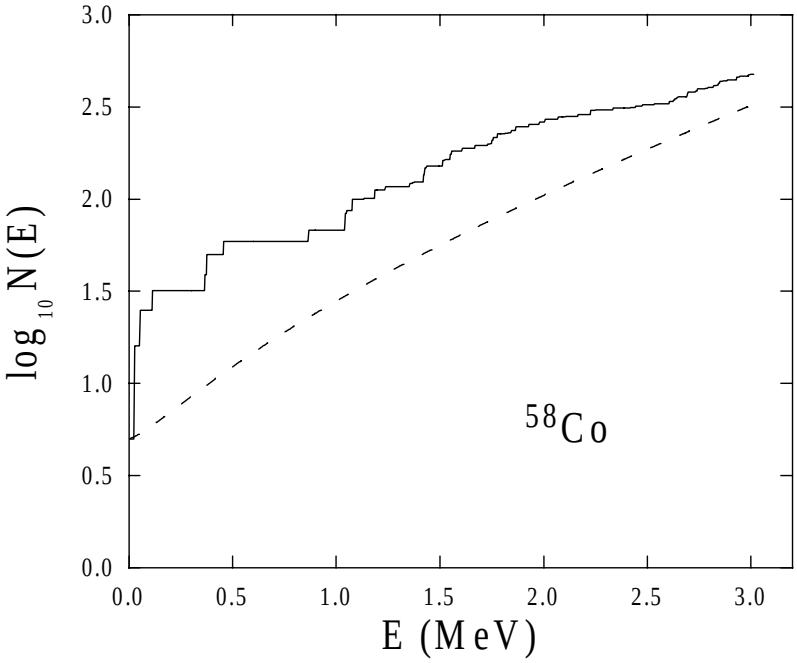

Figure 17
Dimarco et al.

FIG. 17. The same as in Fig. 16 for the ^{58}Co

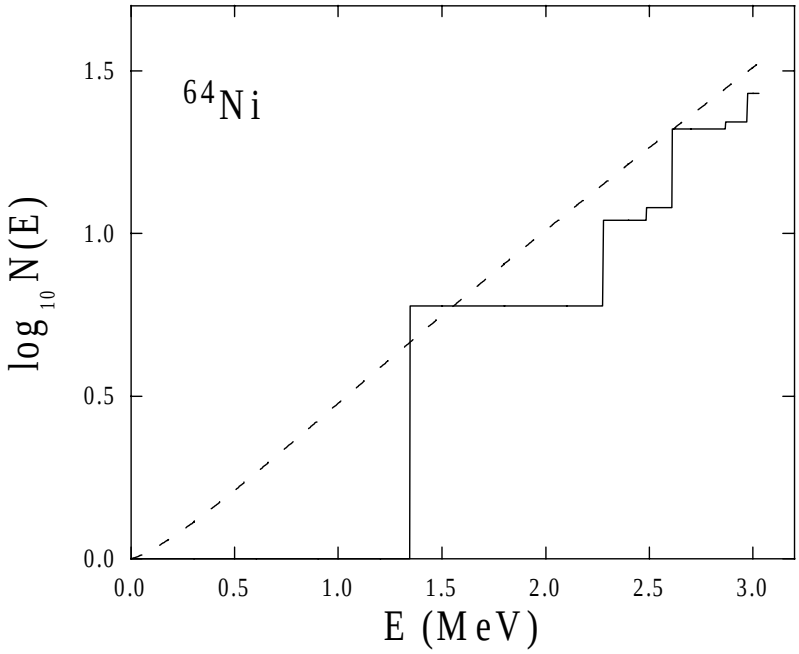

Figure 18
Dimarco et al.

FIG. 18. The same as in Fig. 16 for the ^{64}Ni

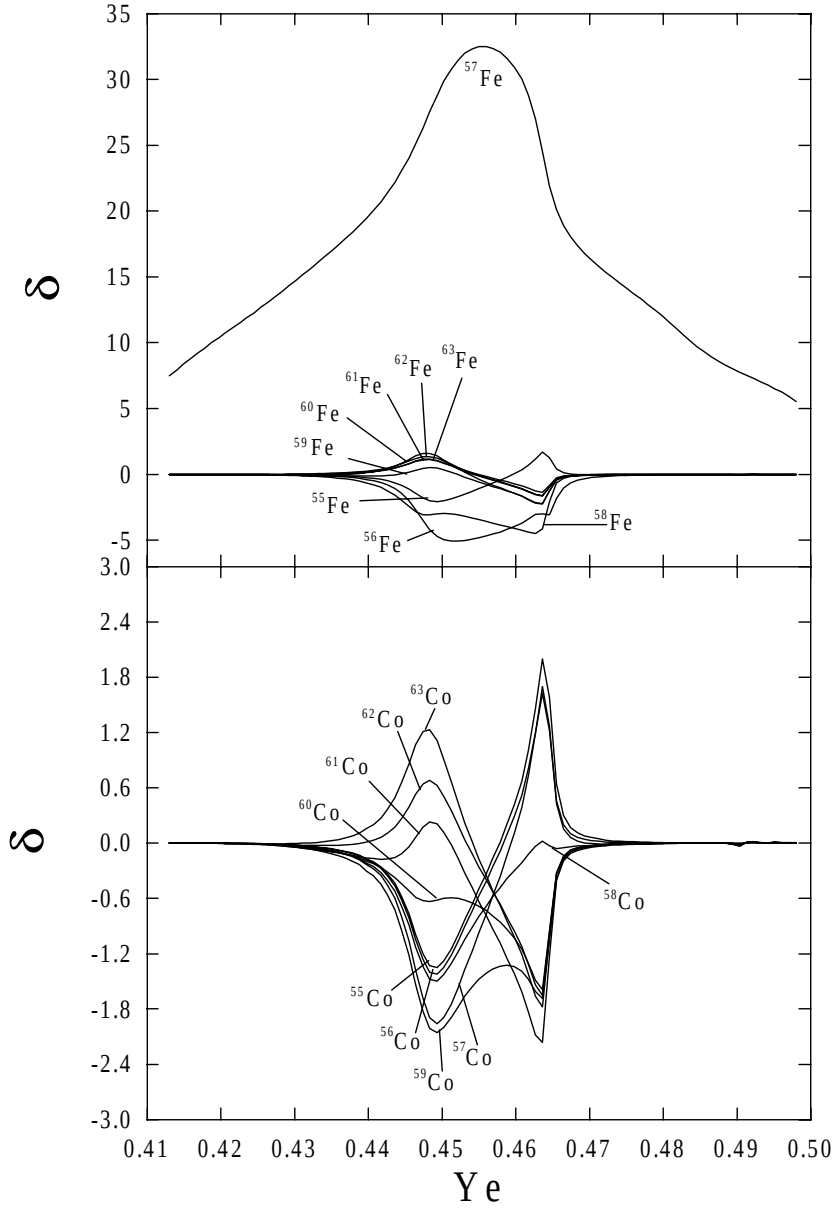

Figure 19
Dimarco et al.

FIG. 19. The parameter $\delta_{A,Z}$ vs. electron fraction for $^{55, 56, 57, 58, 59, 60, 61, 62, 63}$Fe (top graphic) and $^{55, 56, 57, 58, 59, 60, 61, 62, 63}$Co (button graphic).

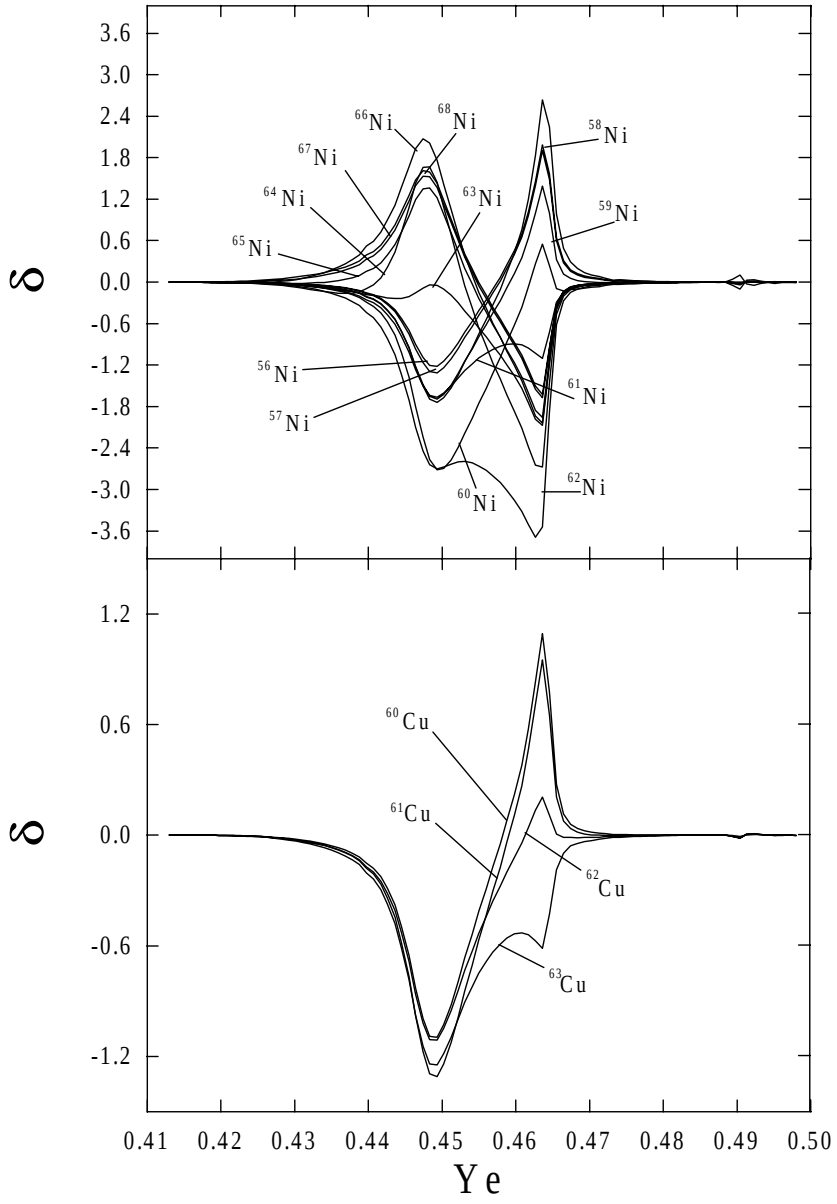

Figure 20
Dimarco et al.

FIG. 20. The same as in Fig. 19 for $^{56,\ 57,\ 58,\ 59,\ 60,\ 61,\ 62,\ 63,\ 64,\ 65,\ 66,\ 67,\ 68}$Ni (top graphic) and $^{60,\ 61,\ 62,\ 63}$Cu (button graphic).

[1] E. M. Burbidge, G. R. Burbidge, W. A. Fowler and F. Hoyle, Rev. Mod. Phys. 29, 547 (1957)

[2] F.-K. Thielemann, F. Brachwitz, C. Freiburghaus, E. Kolbe, G. Martinez-Pinedo, T. Rauscher, F. Rembges, W. R. Hix, M. Liebendoerfer, A. Mezzacappa, K.-L. Kratz, B. Pfeiffer, K. Langanke, K. Nomoto, S. Rosswog, H. Schatz and M. Wiescher Prog. Nuc. Part. Phys., 46, 5 (2000).

[3] K. Nomoto, M. Hashimoto, T. Tsujimoto, F.-K. Thielemann, N. Kishimoto, Y. Kubo and N. Nakasato, Nucl. Phys. A616, 79 (1997).

[4] A. Heger, S. E. Woosley and N. Langer, N. Astr. Rev. 44, 297 (2000)

[5] A. Heger, S. E. Woosley, T. Rausher, R. D. Hoffman and M. M. Boyes, to appear in "Astronomy with Radioactivities III", N. Astr. Rev., (astro-ph/0110015)

[6] H. A.Bethe, G. E. Brown, J. Applegate and J. M. Lattimer, Nucl. Phys. A324, 487 (1979).

[7] F. E. Clifford and R. J. Tayler, MmRAS, 69, Pt2, 21. (1965).

[8] R. I. Epstein and W. D. Arnett, Ap. J. 201, 202 (1975).

[9] M. F. El Eid and W. Hillebrandt, A. and AS.42, 215 (1980).

[10] D. H. Hartman, S. H. Woosley and M. F. El Eid, Ap.J. 297, 837 (1985).

[11] F. Hoyle, Mon Not. R. Astron. Soc. 106,343 (1946).

[12] W. R. Hix and F.-K. Thielemann, Ap.J. 460, 869 (1996).

[13] M. B. Aufderheide, I. Fushiki, S. E. Woosley and D. H. Hartmann, Ap. J. Suppl. 91, 389 (1994).

[14] K. Kar, A. Ray and S. Sarkar, Ap. J. 434, 662 (1994).

[15] M. J. Murphy, Ap. J. Series 42, 385 (1980).

[16] G. M. Fuller, Ap. J. 252, 741 (1982).

[17] H. A. Bethe, Phys. Rev. 50, 332 (1936).

[18] H. A. Bethe, Rev. Mod. Phys. 9, 69 (1937).

[19] T. Von Egidy, A. N. Behkami and H. H. Schmidt, Nucl. Phys. A454, 109 (1986).

[20] F. Garcia, H. O. Rodriguez, P. E. Garrote and T. E. Lopez, J. Phys. G: Nucl. Part. Phys. 19, 2157 (1993).

[21] A. Dimarco, H. Dias, F. Garcia and L. Losano Inter. J. of Mod. Physics E. Vol 9, No 4, 1 (2000).

[22] J. J. Cowan, F.-K. Thielemann and W. Truran, Phys. Rep. 208, 268 (1991).

[23] G. Audi and A. H. Wapstra, Nucl. Phys. A595, 409 (1995).

[24] A. Gilbert and A. G. W. Cameron, Canadian J. Phys. 43, 1446 (1965).

[25] A. Heger, K. Langanke, G. Martínez-Pinedo, S. E. Woosley, Phys. Rev. Lett. 86, 1678 (2001)

[26] G.M. Fuller, W.A. Fowler and M.J. Newman, Ap. J. 42 447 (1980); 48 279 (1982); 252 715 (1982); 293 1 (1985).

[27] M.B. Aufderheide, Nucl. Phys. A526 161 (1991).

[28] M.B. Aufderheide, S.D. Bloom, D.A. Ressler and G.J. Mathews, Phys. Rev. C 47 2961 (1993).

[29] M.B. Aufderheide, S.D. Bloom, D.A. Ressler and G.J. Mathews, Phys. Rev. C 48 1677 (1993).

[30] M.B. Aufderheide, S.D. Bloom, G.J. Mathews and D.A. Ressler, Phys. Rev. C 53 3139 (1996).

[31] D.J. Dean, K. Langanke, L. Chatterjee, P.B. Radha and M.R. Strayer, Phys. Rev. C 58 536 (1998).

[32] E. Caurier, K. Langanke, G. Martínez-Pinedo and F. Nowacki, Nucl. Phys. A653 439 (1999).